System Performance of Cooperative NOMA V2X Network Under Nakagami-*m* Fading Channel

Van Truong Truong[1,2,#] and Dac Binh Ha[1,2]

1 Faculty of Electrical-Electronic Engineering, Duy Tan University, Da Nang, 550000, Vietnam
2 Institute of Research and Development, Duy Tan University, Da Nang, 550000, Vietnam
Corresponding Author / E-mail: truongvantruong@dtu@edu.vn

KEYWORDS: Vehicle-to-Everything, non-orthogonal multiple access, Nakagami-m fading, multi-antenna, cooperative communication

This study investigates a cooperative non-orthogonal multiple access (NOMA) scheme in Vehicle-to-Everything (V2X) network under the Nakagami-m fading channel. Specifically, a multi-antenna road site unit (RSU) communicates with two single-antenna vehicle units (VUs) using downlink non-orthogonal multiple access (NOMA) technique. Furthermore, the near VU can assist in relaying information to the far VU in imperfect channel states and imperfect decoding. We propose two operating protocols for the system based on the RSU's transmit antenna selection. Accordingly, we present two lemmas describing the closed-form expression of the outage probability of two VUs. Finally, we investigate the performance of VUs according to the system parameters such as transmit power, power allocation coefficient, channel fading factor, imperfect factors. The numerical simulation results are entirely consistent with the theoretical calculations, proving the correctness of our study.

Manuscript received: September, 2021 / Revised: January 01, 2022 / Accepted: February 15, 2022

1. Introduction

In recent years, the development of the next-generation wireless network, i.e., 5G or beyond 5G, has enhanced its functionality and broadened its applicability to many existing technologies, including vehicle-to-vehicle connection technology (V2X) [1-2]. V2X is built as an in-car customization network and is a particular part of the Mobile Ad-hoc network. V2X includes wireless communication devices between vehicle units (VU), fixed roadside units (RSU), establishing a network in which all devices can transmit, communicate and share information with extremely low latency [3]. It can be seen that this is a very potential application to help vehicles, especially self-driving cars, get information about traffic, traffic jams, accidents warning, or other instant problems announcement [4-5].

NOMA scheme has recently emerged as a multiple access technique for 5G networks due to it can compromise system performance and users' fairness compared to the orthogonal multiple access (OMA) techniques, i.e., FDMA or TDMA, while exploiting much higher spectral efficiency [6-9]. Moreover, NOMA supports a considerable number of users with high speed and low latency. Islam et al. [7] presented opportunities and challenges in implementing the NOMA model in the 5G network. The authors present successive interference cancelation (SIC) and superposition coding (SC) theoretical basis in terms of outage probability (OP), total user throughput, and spectral efficiency.

Physical layer techniques are also integrated with NOMA in many application scenarios and requirements [8-13]. The concept of the cooperative NOMA was developed by Do et al. present in [8], where near users support forwarding signals to far users to ensure QoS of the system. Furthermore, the concept of cooperative NOMA is very effectively applied in the device-to-device (D2D) communication models [9-10]. Zhao et al. [9] presented a NOMA D2D network, in which users can communicate with the base station (BS) and with each other to improve spectrum efficiency. Specifically, the authors investigated the uplink NOMA D2D network for multiple users communicating with a single antenna BS. A similar model was proposed in [10], with NOMA D2D network applied to IoT scenarios. Thus, it can be seen that the application of the cooperative NOMA technique helps to improve the coverage, capacity, and spectrum efficiency of the network [11-13]. As a further advance, the related works on cooperative NOMA and cooperative NOMA V2X are surveyed exhaustively in the following two paragraphs.

a) Related works on cooperative NOMA: The cooperative NOMA wireless communications have sparked a lot of attention [14-16]. Budhiraja [14] proposed a cooperative NOMA model, in which center users can harvest radio frequency energy to decode and forward data to the far users. The authors investigated the system under the imperfectly estimated Rayleigh channel. However, the authors have not explained whether perfect SIC decoding at the devices is consistent with reality. Unlike the previous studies, in [15] and [16], the authors investigated the cooperative NOMA network for the uplink. Kader et al. [16] proposed a two-user cooperative NOMA model for the uplink. The two central users can communicate directly with the BS and support the edge users through D2D communication. The results have shown that the proposed model achieves a much higher total throughput than the traditional OMA model. However, the authors investigated the system under the Rayleigh transmission channel and single-antenna device quite simply.

b) Related works on cooperative NOMA-V2X: From the above surveys, it can be seen that the application of the cooperative NOMA technique to the V2X network is a potential solution to help solve communication problems in this network [17-20]. The results obtained in the study [18] by Liu et al. confirmed that the collaborative V2X NOMA network achieves high spectral efficiency and very low communication latency. In [19], downlink NOMA can apply to communicate between RSUs and VUs, while D2D communication in NOMA networks ensures VUs can exchange data with each other. Ihsan et al. [20] proposed an energy-efficient RSUs assisted NOMA

multicasting system for 5G cellular V2X communications. The authors proposed complexity optimal power allocation algorithms for multicasting the information under channel outage probability constraints of vehicles with imperfect CSI. The channel outage probability constraint has formulated a problem as a nonconvex probabilistic optimization problem and solved by converting the probabilistic problem through relaxation into a non-probabilistic problem.

To the best of our knowledge, studies on the application of cooperative NOMA networks in V2X networks are very sparse. Furthermore, the impact of imperfect channel state information (ipCSI) and imperfect successive interference cancellation (ipSIC) in the NOMA V2X network have also not been considered. Unlike existing works of literature, in this work we propose the NOMA V2X network model where multi-antenna RSU communicates with two VU under the Nakagami-m fading channel under the condition of ipCSI and ipSIC. The main contributions of this study are listed as follows:

• Propose a V2X network model using the NOMA cooperation technique under Nakagami-m transmission channel in ipCSI and ipSIC conditions. Specifically, a multi-antenna RSU will communicate with two VUs using downlink NOMA. The near VU acts as a decoder and data relay for the far VU.

• Derive the closed-form expression of the outage probability (OP) of each VU according to two proposed schemes, namely TAS1 and TAS2, according to essential network parameters such as transmit power, power allocation coefficient, channel fading factor, ipSIC factor, ipCSI factor, and the distance between VUs.

• The performance of the system is investigated using Monte-Carlo simulation. The results show that the performance of VUs can be improved by choosing the optimal power allocation coefficient.

The structure of the paper is presented as follows: Section II presents the system model and communication protocol. Section III presents the performance analysis of the proposed system. Section IV describes the numerical results and discussion. Section V is the conclusion and future work of the paper.

2. System model and protocol

2.1 System model

In this study, we investigate a cooperative NOMA system for downlink in a V2X network, as depicted in Figure 1. A multi-antenna fixed road side unit (RSU) communicates with two vehicle units (VUs), denoted by VU1 and VU2, respectively. Assuming VU1 is closer to the RSU than VU2, both are equipped with a single antenna, move towards the RSU, and the equipped transceiver circuits operate in half-duplex.

Let K be the number of antennas at the *RSU*. Let h_{k1}, h_{k2}, h_3 be the channel coefficient of transmission from antenna k of *RSU* to VU_1, from antenna k of *RSU* to VU_2, and from VU_1 to VU_2, respectively. The channel coefficients $h_X, X \in \{k1, k2, 3\}$ in the proposed system are modeled as random variables following the Nakagami-*m* distribution.

Since the channel estimation process gets the error, we consider the imperfect channel state information (ipCSI) case, h_X with fading factor m_X is modeled as $h_X = \hat{h}_X + e_X$. Where $\hat{h}_X$ is the estimated channel coefficient, $e_X \sim CN\left(0, \sigma_X^2\right)$ describes the channel estimation error and is a random variable that follows a Gaussian distribution with zero mean and variance σ_X^2.

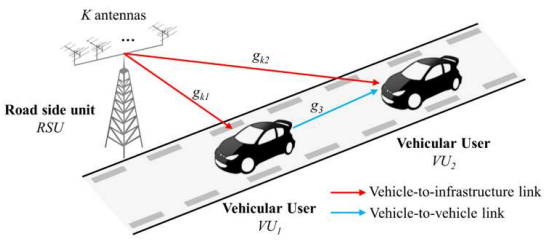

Fig. 1 System model for downlink cooperative V2X-NOMA communication

Let d_{k1}, d_{k2}, d_3 be the distance from antenna k of *RSU* to VU_1, from antenna k of *RSU* to VU_2, and from VU_1 to VU_2, respectively, $1 \le k \le K$, α be the path loss coefficient. We have the random variable's mean describing the channel gain $|h_X|^2$ as $E\left(|h_X|^2\right) = \Omega_X = d_X^{-\alpha}$. Since $\hat{h}_X$ and e_X are statistically independent, we have the estimated link average power of $|h_X|^2$ is $\hat{\Omega}_X = \Omega_X - \sigma_{e_X}^2$. Let $\eta_X = \sigma_X^2 / \Omega_{X_\alpha}$ be the relative channel estimation error, we have $\sigma_{e_X}^2 = \eta_X d_X^{\alpha}$. Note that we obtain the perfect channel state information case (pCSI) when $\eta_X = 0$.

2.2 System protocol

In the proposed model, VU_1 communicates directly with *RSU*, while VU_2 can communicate with the *RSU* directly or through a relay from VU_1. We continue to present a two-phase operation protocol for the proposed system with specific mathematical expressions.

In the first phase, the *RSU* broadcasts the signal directly to VU_1 and VU_2 using downlink NOMA. Assume that *RSU* selects an antenna k^* for communication. The received signal at VU_1 and VU_2 from k^* are as follow:

$$y_1 = \left(\sqrt{\rho P}x_1 + \sqrt{(1-\rho)P}x_2\right)\left(\hat{h}_{k^*1} + e_1\right) + n_1, \quad (1)$$

$$y_2 = \left(\sqrt{\rho P}x_1 + \sqrt{(1-\rho)P}x_2\right)\left(\hat{h}_{k^*2} + e_2\right) + n_2. \quad (2)$$

where P is the transmit power of the RSU, ρ is the power allocation coefficient, x1 and x2 are the signals sent to VU1 and VU2, respectively, n1 and n2 are the additive white Gaussian noise (AWGN) with zero mean and variance σ_0^2, i.e., $n_i \sim CN\left(0, \sigma_0^2\right)$, $i \in \{1,2\}$.

VU_1 closer to the *RSU*, thus it has the better channel condition than will be allocated less power to ensure fairness among users in the network, i.e., $0 < \rho < 0.5$. So, applying the NOMA technique, signal x_2 is decoded first at VU_1. The SINR at VU_1 used to decode signal x_2 is:

$$\gamma_1^{x_2} = \frac{(1-\rho)\gamma_0 \hat{g}_{k^*1}}{\rho\gamma_0 \hat{g}_{k^*1} + \eta_1 d_1^{-\alpha}\gamma_0 + 1} = \frac{(1-\rho)\gamma_0 \hat{g}_{k^*1}}{\rho\gamma_0 \hat{g}_{k^*1} + a_1}, \quad (3)$$

where $\gamma_0 = \frac{P}{\sigma_0^2}$, $a_1 = \eta_1 d_1^{-\alpha}\gamma_0 + 1$.

Due to the effect of imperfect successive interference cancellation (ipSIC), the x_2 signal is not entirely decoded and becomes an interference component affecting the x_1 signal decoding process. Thus, the SINR at VU_1 used to decode signal x_1 is:

$$\gamma_1^{x_1} = \frac{\rho\gamma_0\hat{g}_{k^*1}}{\kappa\gamma_0\hat{g}_{k^*1} + \eta_1 d_1^{-\alpha}\gamma_0 + 1} = \frac{\rho\gamma_0\hat{g}_{k^*1}}{\kappa\gamma_0\hat{g}_{k^*1} + a_1}, \quad (4)$$

where κ is a coefficient describing the residual interference signal coefficient after the SIC process. Note that when $\kappa = 0$, we got the perfect SIC (pSIC) case.

In *VU2*, since x_2 is allocated a higher power level than x_1, x_2 is decoded first. The SINR at *VU2* used to decode signal x_2 is:

$$\gamma_2 = \frac{(1-\rho)\gamma_0\hat{g}_{k^*2}}{\rho\gamma_0\hat{g}_{k^*2} + \eta_2 d_2^{-\alpha}\gamma_0 + 1} = \frac{(1-\rho)\gamma_0\hat{g}_{k^*2}}{\rho\gamma_0\hat{g}_{k^*2} + a_2}, \quad (5)$$

với $a_2 = \eta_2 d_2^{-\alpha}\gamma_0 + 1$

In the second phase, *VU1* forwards data to *VU2*. Suppose *VU1* uses a decoding and forwarding (DF) technique to transmit the signal to *VU2*. The received signal at *VU2* in this phase is:

$$y_{1\to 2} = \left(\sqrt{P_1}x_2\right)\left(\hat{h}_3 + e_3\right) + n_3. \quad (6)$$

where P_1 is the transmit power of *VU1*, n_3 are the AWGN with zero mean and variance σ_0^2, i.e., $n_3 \sim CN\left(0, \sigma_0^2\right)$

Without loss of generality, we assume $P_1 = P$. Then, the SINR of *VU2* to decode x_2 in second phase is:

$$\gamma_{1\to 2} = \frac{\gamma_0\hat{g}_3}{\eta_3 d_3^{-\alpha}\gamma_0 + 1} = \frac{\gamma_0\hat{g}_3}{a_3}, \quad (7)$$

where $a_3 = \eta_3 d_3^{-\alpha}\gamma_0 + 1$.

VU2 uses the MRC mechanism to incorporate signals to get better SNR. Thus, the SNR at *VU2* for decoding x_2 is:

$$\gamma_2^{MRC} = \gamma_2 + \gamma_{1\to 2} = \frac{(1-\rho)\gamma_0\hat{g}_{k^*2}}{\rho\gamma_0\hat{g}_{k^*2} + a_2} + \frac{\gamma_0\hat{g}_3}{a_3}, \quad (8)$$

Before the communication process takes place, the *RSU* collects channel information of the entire system, thereby selecting antennas to send the signal. We propose two antenna selection schemes, named TAS1 and TAS2, as follows:

a. TAS1 scheme

In the TAS1 scheme, the *RSU* chooses k^* to maximize the SINR at *VU1*. Note that the forwarding activity of *VU1* plays an essential role in the operation of the proposed system, so this scheme ensures that *VU1* achieves the most advantageous conditions for communication. The mathematical expression describing the antenna selection in the TAS1 mechanism is presented as follows:

$$\begin{aligned} k^* &= \arg\max_{1\le k\le K}\left(\gamma_1^{x_1}, \gamma_1^{x_2}\right) \\ &= \arg\max_{1\le k\le K}\left(\frac{\rho\gamma_0\hat{g}_{k1}}{\kappa\gamma_0\hat{g}_{k1} + a_1}, \frac{(1-\rho)\gamma_0\hat{g}_{k1}}{\rho\gamma_0\hat{g}_{k1} + a_1}\right), \\ &= \arg\max_{1\le k\le K}\hat{g}_{k1} \end{aligned} \quad (9)$$

b. TAS2 scheme

In the TAS2 scheme, *RSU* chooses k^* in order to maximize the achievable channel capacity of *VU2*, called C_{VU_2}.

$$C_{VU_2} = \min\left\{\log_2\left(1+\gamma_1^{x_2}\right), \log_2\left(1+\gamma_2\right)\right\}. \quad (10)$$

In the proposed system, since *VU1* is much closer to *RSU* than *VU2*, so (10) can be approximated as follows:

$$C_{VU_2} = \log_2\left(1+\gamma_2\right). \quad (11)$$

Thus, the formula describing the antenna selection for the TAS2 scheme is:

$$\begin{aligned} k^* &= \arg\max_{1\le k\le K}\left(\gamma_2\right) \\ &= \arg\max_{1\le k\le K}\frac{(1-\rho)\gamma_0\hat{g}_{k2}}{\rho\gamma_0\hat{g}_{k2} + a_2}. \\ &= \arg\max_{1\le k\le K}\hat{g}_{k2} \end{aligned} \quad (12)$$

According to the proposed schemes, we describe the PDF and CDF of the channel power gain according to the following formulas.

CDF of $\hat{g}_X$:

$$F_{\hat{g}_X}(x) = \sum_{k=0}^{K}\sum_{\Delta_{tasX}=k}\Phi_{tasX}.x^{\varphi_{tasX}}.\exp\left(-k\delta_X x\right), \quad (13)$$

PDF of $\hat{g}_X$:

$$f_{\hat{g}_X}(x) = \sum_{k=0}^{K}\sum_{\Delta_{tasX}=k}\Phi_{tasX}\left(\varphi_{tasX}.x^{\varphi_{tasX}-1}.\exp\left(-k\delta_X x\right) - k\delta_X x^{\varphi_{tasX}}.\exp\left(-k\delta_X x\right)\right) \quad (14)$$

CDF of $\hat{g}_Y$:

$$F_{\hat{g}_Y}(x) = 1 - \sum_{i=0}^{m_Y-1}\frac{1}{i!}\delta_Y^i x^i\exp\left(-\delta_Y x\right), \quad (15)$$

PDF of $\hat{g}_Y$:

$$f_{\hat{g}_Y}(x) = \frac{\delta_Y^{m_Y}.x^{m_Y-1}}{\Gamma\left(m_Y\right)}\exp\left(-\delta_Y x\right), \quad (16)$$

where $\delta_X = \frac{m_X d_X^{\alpha}}{1-\eta_X}$, $X \in \begin{cases}\{1\} & ,TAS1\\ \{2\} & ,TAS2\end{cases}$,

$Y \in \begin{cases}\{2,3\} & ,TAS1\\ \{1,3\} & ,TAS2\end{cases}$

$$\Phi_{tasX} = \binom{K}{k}\binom{k}{\sigma_0,\ldots,\sigma_{m_X-1}}(-1)^k\left[\prod_{j=0}^{m_X-1}\left(\frac{\delta_X^j}{j!}\right)^{\sigma_j}\right],$$

$$\Delta_{tasX} = \sum_{j=0}^{m_X-1}\sigma_j,\ \varphi_{tasX} = \sum_{j=0}^{m_X-1}j\delta_j.$$

3. Performance analysis

In this section, we analyze the system performance of the downlink cooperative NOMA networks with ipCSI and ipCSI under Nakagami-*m* fading channels in terms of the outage probability (OP). The OP of *VU*s is defined as the probability that the instantaneous data rate is less than a given threshold. Let R_{th1} and R_{th2} be the data rates of *VU1* and *VU2*, respectively, whereby $\gamma_{th1} = 2^{2R_{th1}} - 1, \gamma_{th2} = 2^{2R_{th2}} - 1$ are the threshold SNR for decoding x_1 and x_2, respectively. According to the two proposed schemes, the OP's of two *VU*s are shown in the two following lemmas.

3.1. OP analysis for *VU1*

The OP of *VU1* is the complement of the probability that *VU1* decodes the signal of both x_1 and x_2. Thus, the OP of *VU1*, denoted by $P_{out}^{VU_1}$, is given by the formula:

$$P_{out}^{VU_1} = 1 - \Pr\left(\gamma_1^{x_2} \ge \gamma_{th2}, \gamma_1^{x_1} > \gamma_{th1}\right). \quad (17)$$

Lemma 1: The closed-form expression of OP of *VU1* in V2X

system deploying cooperative NOMA technique under Nakagami-*m* channel with the ipCSI and ipSIC conditions is given as follow

$$P_{out}^{VU_1}=\begin{cases}\sum_{k=0}^{K}\sum_{\Delta_{tas1}=k}\Phi_{tas1}.\varphi^{\varphi_{tas1}}.\exp\left(-k\delta_X\varphi\right),\gamma_{th2}<\dfrac{1-\rho}{\rho}\ \&\ \gamma_{th1}<\dfrac{\rho}{\kappa},TAS1\\ 1-\sum_{i=0}^{m_1-1}\dfrac{1}{i!}\delta_1^i\varphi^i\exp\left(-\delta_1\varphi\right),\gamma_{th2}<\dfrac{1-\rho}{\rho}\ \&\ \gamma_{th1}<\dfrac{\rho}{\kappa},TAS2\\ 1,otherwise\end{cases} \quad (18)$$

where $\varphi=\max\left(\varphi_1,\varphi_2\right)$, $\varphi_1=\dfrac{\gamma_{th2}a_1}{\gamma_0\left(1-\rho-\rho\gamma_{th2}\right)}$,

$\varphi_2=\dfrac{\gamma_{th1}a_1}{\gamma_0\left(\rho-\kappa\gamma_{th1}\right)}$.

Proof: See appendix A.

3.2. OP analysis for VU_2

The OP of VU_2 is the probability that VU_1 successfully decodes x_2 in the first phase, but the SINR after VU_2 incorporates the signal from the two phases is lower than the given threshold, or both VU_1 and VU_2 cannot decode the signal x_2. Thus, the mathematical expression describing the OP of VU_2 is:

$$P_{out}^{VU_2}=\Pr\left(\gamma_1^{x_2}>\gamma_{th2},\gamma_2^{MRC}<\gamma_{th2}\right)+\Pr\left(\gamma_1^{x_2}<\gamma_{th2},\gamma_2^{x_2}<\gamma_{th2}\right) \quad (19)$$

Lemma 2: The closed-form expression of OP of VU_2 in V2X system deploying cooperative NOMA technique under Nakagami-*m* channel with the ipCSI and ipSIC conditions is given as follow

$$P_{out}^{VU_2}=AB+C, \quad (20)$$

where

$$A=\begin{cases}1-\exp\left(-\delta_2\varphi_4\right)\sum_{i=0}^{m_2-1}\dfrac{\left(\delta_2\varphi_4\right)^i}{i!}-\sum_{i=0}^{m_2-1}\dfrac{\delta_3^i}{i!}\dfrac{\delta_2^{m_2}}{\Gamma\left(m_2\right)}\dfrac{\pi}{2Q}\varphi_4\sum_{q=1}^{Q}\left[\varphi_3-\dfrac{\left(1-\rho\right)a_3x_q}{\rho\gamma_0x_q+a_2}\right]^i x_q^{m_2-1}\\ x\exp\left(-\delta_3\left(\varphi_3-\dfrac{\left(1-\rho\right)a_3x_q}{\rho\gamma_0x_q+a_2}\right)-\delta_2x_q\right)\sqrt{1-\phi_q^2}, \quad TAS1\\ 1-\sum_{k=1}^{K}\sum_{\Delta tas2=k}\Phi_{tas2}\left(k\delta_2\right)^{-\varphi_{tas2}}\left(\varphi_{tas2}\Gamma\left(\varphi_{tas2},k\delta_2\varphi_4\right)-\Gamma\left(\varphi_{tas2}+1,k\delta_2\varphi_4\right)\right)\\ -\sum_{i=0}^{m_1-1}\dfrac{\delta_3^i}{i!}\sum_{k=0}^{K}\sum_{\Delta_{tas2}=k}\Phi_{tas2}\dfrac{\pi}{2Q}\varphi_4\sum_{q=1}^{Q}\left[\varphi_3-\dfrac{\left(1-\rho\right)a_3x_q}{\rho\gamma_0x_q+a_2}\right]^i\left(\varphi_{tas2}.x_q^{\varphi_{tas2}-1}-k\delta_2x_q^{\varphi_{tas2}}\right)\\ x\exp\left[-\delta_3\left(\varphi_3-\dfrac{\left(1-\rho\right)a_3x_q}{\rho\gamma_0x_q+a_2}\right)-k\delta_2x_q\right]\sqrt{1-\phi_q^2}, \quad TAS2\end{cases}$$

$$B=\begin{cases}0,\gamma_{th2}>\dfrac{1-\rho}{\rho}\\ 1-\sum_{k=0}^{K}\sum_{\Delta_{tas1}=k}\Phi_{tas1}.\varphi_1^{\varphi_{tas1}}.\exp\left(-k\delta_1\varphi_1\right),\gamma_{th2}>\dfrac{1-\rho}{\rho}, \quad TAS1\\ \sum_{i=0}^{m_1-1}\dfrac{1}{i!}\delta_1^i\varphi_1^i\exp\left(-\delta_1\varphi_1\right),\gamma_{th2}>\dfrac{1-\rho}{\rho}, \quad TAS2\end{cases},$$

$$C=\begin{cases}1,\gamma_{th2}>\dfrac{1-\rho}{\rho}\\ \sum_{k=0}^{K}\sum_{\Delta_{tas1}=k}\Phi_{tas1}.\varphi_1^{\varphi_{tas1}}.\exp\left(-k\delta_1\varphi_1\right)\left[1-\sum_{i=0}^{m_1-1}\dfrac{1}{i!}\delta_2^i\varphi_4^i\exp\left(-\delta_2\varphi_4\right)\right],\gamma_{th2}<\dfrac{1-\rho}{\rho}, \quad TAS1\\ \left[1-\sum_{i=0}^{m_1-1}\dfrac{1}{i!}\delta_1^i\varphi_1^i\exp\left(-\delta_1\varphi_1\right)\right]\sum_{k=0}^{K}\sum_{\Delta_{tas1}=k}\Phi_{tas2}.\varphi_4^{\varphi_{tas2}}.\exp\left(-k\delta_2\varphi_4\right),\gamma_{th2}<\dfrac{1-\rho}{\rho}, \quad TAS2\end{cases}$$

$\varphi_3=\dfrac{\gamma_{th2}a_3}{\gamma_0}$, $\varphi_4=\dfrac{\gamma_{th2}a_2}{\gamma_0\left(1-\rho-\rho\gamma_{th2}\right)}$, $\phi_q=\cos\left(\dfrac{2q-1}{2Q}\pi\right)$,

$x_q=\dfrac{\phi_q+1}{2}\varphi_4$; Q is the complexity-vs-accuracy trade-off coefficient.

Proof: See appendix B.

4. Numerical results and discussion

In this section, we present numerical results and discuss the system performance of *VU*s in terms of OP. The parameters using in Monte-Carlo simulation are given in Table 1. We consider that the *RSU*, VU_1, and VU_2 are located in a straight line. Without loss of generality, assume that the distance between *RSU* and VU_2 is normalized to unity, and we can acquire $d_3 = 1 - d_1$, where d_1 and d_3 are the normalized distance between the *RSU* and VU_1, and between VU_1 and VU_2, respectively.

Table 1 Simulation parameter

Parameter	Notation	Typical Values
Environment		Nakagami-*m*
Fading parameter	m_1, m_2, m_3	2, 2, 3
The distance form *RSU* - VU_1	d_1	0.01-1
The distance form *RSU* - VU_2	d_2	1
The distance form VU_1 - VU_2	d_3	1-d_1
Path loss exponent	α	2
Transmit power of the *RSU* and VU_1	P	0-30 dB
Number of antennas of *RSU*	K	2
ipCSI factor	η	0.002
ipSIC factor	κ	0.06
Power allocation coefficient	ρ	0.2
Threshold data rate	R_{th1}, R_{th2}	0.8

In this experiment, we consider the effect of the power allocation coefficient (ρ) on the performance of *VU*s, depict as Fig. 2. The curves describing the performance of VU_1 in both schemes have similar form. When ρ has a minor value, OP reaches a considerable value, i.e., poor performance. OP decreases and reaches a minimum value when ρ increases. Finally, OP increases again when ρ is too large. Thus, there exists a power allocation coefficient such that the performance of VU_1 is optimal. The following observation explicates that the performance of VU_1 when the system uses the TAS1 scheme is better than when the system uses the TAS2 scheme.

As for the performance of VU_2, both schemes show a gradual decline in performance as ρ increases. It is consistent that as ρ increases, the power allocated to VU_2 decreases, leading the increasing of OP.

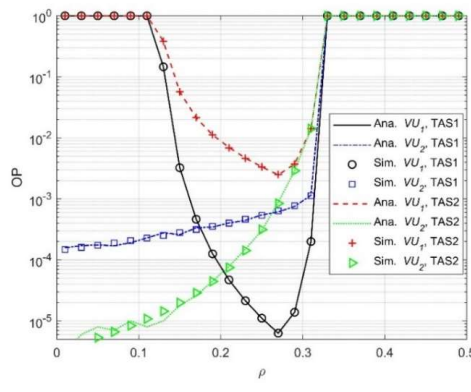

Fig. 2 The impact of power allocation coefficient on OP of VUs under two schemes

We continue investigate the system performance considering the effect of average transmit SNR (γ_0) , as Fig. 3. The results show that the OP of the *VU*s decreases when γ_0 increases. In other words, when the transmit power is increased, the system performance of the *VU*s improves. When γ_0 increases, there is a tendency to saturation of $P_{out}^{VU_1}$. The two schemes, i.e., TAS1 and TAS2, prioritize choosing the best channel for the link from *RSU* to VU_1 and VU_2, respectively, so the OP of VU_1 in TAS1 scheme is better than TAS2 scheme and vice versa, the OP of VU_2 in TAS2 scheme is better than in TAS1.

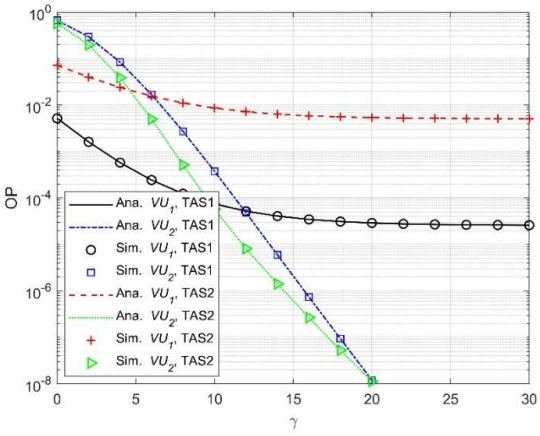

Fig. 3 The impact of average transmit power on OP of VUs under two schemes

In this experiment, we consider the effect of the distance from *RSU* to VU_1 (d_1) on system performance. Fig. 4 shows that when d_1 increases, the performance of VU_1 declines in both schemes. Observing the performance of VU_2, we notice that OP gradually decreases and reaches the minimum value, and then gradually increased when d_1 increased from 0.01 to 1.

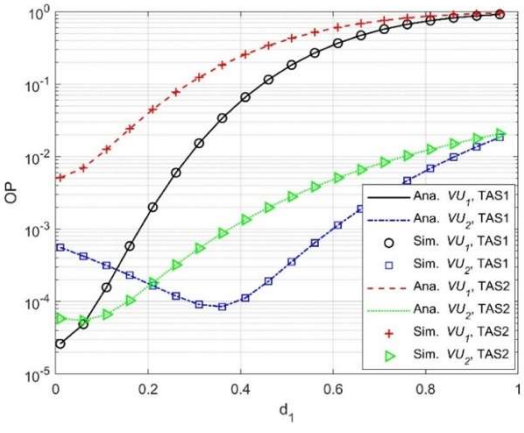

Fig. 4. The impact of distance of RSU-VU_1 on performance of VUs under two schemes

Fig. 5 (a) and (b) investigate the effects of ipCSI (η) and ipSIC (κ) coefficients on OP of *VU*s by two schemes. In both schemes, we consider two scenarios, the first one (i) ipCSI ($\eta = 0.002$), ipSIC ($\kappa = 0.06$) and the second one (ii) pCSI ($\eta = 0$), pSIC ($\kappa = 0$). Note that scenario (ii) indicates that the OP of the *VU*s is optimal and is obtained only under ideal conditions. Therefore, the proposed model under scenario (i) is suitable for real conditions and can give a more accurate view of the system's behavior. As the coefficients increase, the OP of the *VU*s increases in both cases, meaning the system performance decreases.

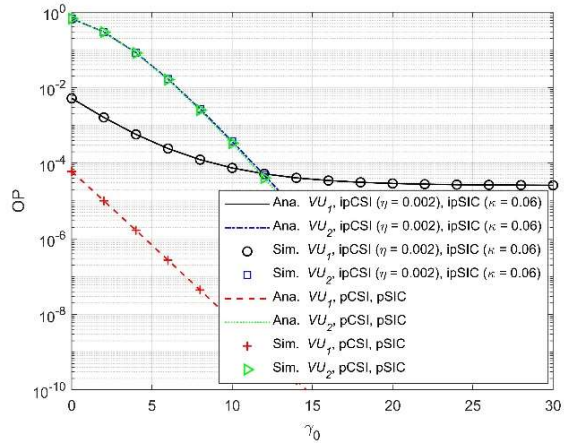

Fig. 5(a)

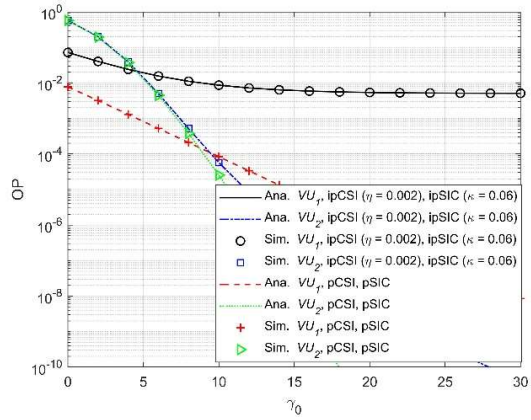

Fig. 5(b)

Fig. 5 The impact of ipCSI factor and ipSIC on performance of VUs,

(a) TAS1 scheme, (b) TAS2 scheme

Figs. 6 (a) and (b) investigate the number of *RSU* antennas (*K*) on OP of *VU*s in two schemes. For the TAS1 scheme, Fig. 6a shows that the impact of *K* on the OP of VU_1 is evident: *K* increases allow $P_{out}^{VU_1}$ to decrease. It is consistent with the fact that when increasing the number of antennas at the *RSU*, the probability of the system choosing the best transmission channel from the *RSU* to the VU_1 will be higher, thereby increasing the performance of the VU_1. Meanwhile, this impact only affects the performance of VU_2 as average transmits power increases. The same thing happens in the TAS2 scheme; *K* increases to help $P_{out}^{VU_2}$ decrease. However, the number of antennas in the *RSU* does not affect the performance of VU_1 in this scheme. It is entirely consistent with the theoretical calculation in the formula (18).

The results from Fig. 2 to Fig. 6 show that the theoretical simulation (Sim.) and computational analysis (Ana.) completely coincide, proving the correctness of our study.

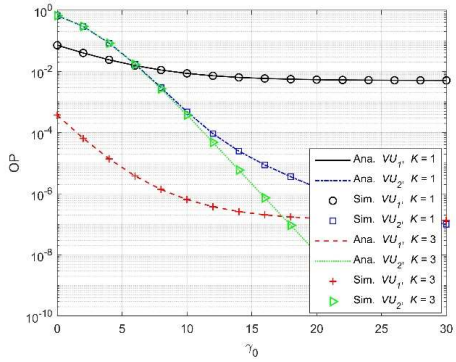

Fig. 6(a)

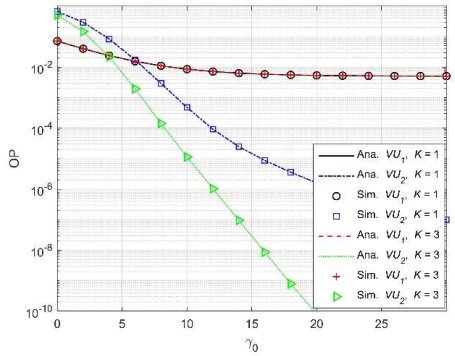

Fig. 6(b)

Fig. 6 The impact of the number of antennas of RSU on performance of VUs,

(a) TAS1 scheme, (b) TAS2 scheme

5. Conclusion and future work

In this study, we have investigated a two-user V2X system communicating with a multi-antenna RSU under the Nakagami-*m* transmission channel using the cooperative NOMA technique. We have proposed two protocols for system operation based on *RSU*'s transmit antenna selection under ipCSI and ipSIC conditions. Accordingly, the closed-form expressions for the outage probability of two *VU*s in the network are derived and used these criteria to evaluate performance. The results show that choosing the optimal power allocation coefficient, and/or increasing the number of antennas of the RSU can improve the performance of *VU*s. The results of the Monte Carlo simulation coincide with the theoretical calculations that have proven the correctness of this study.

In future work, we investigate the case of *VU*s equipped with multiple antennas and apply optimization algorithms to find the power allocation coefficient so that the OP of *VU*s is the lowest.

REFERENCES

1. Chen, S., Hu, J., Shi, Y., Peng, Y., Fang, J., Zhao, R. and Zhao, L., "Vehicle-to-everything (V2X) services supported by LTE-based systems and 5G," *IEEE Communications Standards Magazine*, vol. 1, no. 2, pp. 70-76, 2017.
2. Naik, G., Choudhury, B. and Park, J., "IEEE 802.11 bd & 5G NR V2X: Evolution of radio access technologies for V2X communications," *IEEE access*, vol. 7, 70169-70184, 2019.
3. Storck, C. and Duarte-Figueiredo, F., "A 5G V2X ecosystem providing internet of vehicles," *Sensors*, vol. 19, no. 3, pp. 550, 2019.
4. Kokuti, A., Hussein,A., Marín-Plaza, P., de La Escalera, A. and García, F., "V2X communications architecture for off-road autonomous vehicles," in Proc. IEEE International Conference on Vehicular Electronics and Safety (ICVES), pp. 69-74, IEEE, 2017
5. Wu, Z., Qiu, K.K. and Gao, H., "Driving policies of V2X autonomous vehicles based on reinforcement learning methods," *IET Intelligent Transport Systems*, vol. 14, no. 5, pp. 331-337, 2020.
6. Wu, Z., Lu, K., Jiang, C. and Shao, X., "Comprehensive study and comparison on 5G NOMA schemes," *IEEE Access*, vol. 6, pp. 18511-18519, 2018.
7. Islam, S., Avazov, N., Dobre, O. and Kwak, K., "Power-domain non-orthogonal multiple access (NOMA) in 5G systems: Potentials and challenges," *IEEE Communications Surveys & Tutorials*, vol. 19, no. 2, pp. 721-742, 2016.
8. Do, N. T., Da Costa, D. B., Duong T. Q. and An, B., "A BNBF User Selection Scheme for NOMA-Based Cooperative Relaying Systems With SWIPT," in *IEEE Communications Letters*, vol. 21, no. 3, pp. 664-667, March 2017, doi: 10.1109/LCOMM.2016.2631606.
9. Zhao, J., Liu, Y., Chai, K., Chen, Y., Elkashlan, M. and Alonso-Zarate, J., "NOMA-based D2D communications: Towards 5G," In Proc. IEEE Global Communications Conference (GLOBECOM) pp. 1-6, IEEE, 2016.
10. Elouafadi, R. and Benjillali, M., "Cooperative NOMA-based D2D communications: A survey in the 5G/IoT context," In Proc. 19th IEEE Mediterranean Electrotechnical Conference (MELECON), pp. 132-137, IEEE, 2018.
11. Do, T. N., da Costa, D. B., Duong, T. Q. and An, B., "Improving the Performance of Cell-Edge Users in MISO-NOMA Systems Using TAS and SWIPT-Based Cooperative Transmissions," in *IEEE Transactions on Green Communications and Networking*, vol. 2, no. 1, pp. 49-62, March 2018, doi: 10.1109/TGCN.2017.2777510.
12. Chen, J., Yang, L., and Alouini, M. S. (2018). Physical layer security for cooperative NOMA systems. *IEEE Transactions on Vehicular Technology*, *67*(5), 4645-4649.
13. Liu, H., Ding, Z., Kim, K. J., Kwak, K. S. and Poor, H. V. (2018). Decode-and-forward relaying for cooperative NOMA systems with direct links. *IEEE Transactions on Wireless Communications*, *17*(12), 8077-8093.
14. Budhiraja, I., Kumar, N., Tyagi, S., Tanwar, S. and Guizani, M., "SWIPT-enabled D2D communication underlaying NOMA-based cellular networks in imperfect CSI," *IEEE Transactions on Vehicular Technology*, vol. 70, no. 1, pp. 692-699, 2021.
15. Xu, Y., Wang, G., Li, B. and Jia, S., "Performance of D2D aided uplink coordinated direct and relay transmission using NOMA," *IEEE Access*, vol. 7, pp. 151090-151102, 2019.
16. Kader, M., Islam, S. and Dobre, O., "Simultaneous Cellular and D2D Communications Exploiting Cooperative Uplink NOMA," *IEEE Communications Letters*, 2021.

17. Song, B. Di, L., Li, Y. and Han, Z., "V2X meets NOMA: Non-orthogonal multiple access for 5G-enabled vehicular networks," *IEEE Wireless Communications*, vol. *24, no.* 6, pp. 14-21, 2017.

18. Liu, G., Wang, Z., Hu, J., Ding, Z. and Fan, P., "Cooperative NOMA broadcasting/multicasting for low-latency and high-reliability 5G cellular V2X communications," *IEEE Internet of Things Journal*, vol. *6,* no. 5, pp. 7828-7838, 2019.

19. Do, D., Nguyen, V., Le, A., Rabie, K. and Zhang, J., "Joint full-duplex and roadside unit selection for NOMA-enabled V2X communications: ergodic rate performance," *IEEE Access*, vol. *8*, pp. 140348-140360, 2020.

20. Ihsan, A., Chen, W., Zhang, S. and Xu, S., "Energy-Efficient NOMA Multicasting System for Beyond 5G Cellular V2X Communications With Imperfect CSI," *IEEE Transactions on Intelligent Transportation Systems*, 2021

APPENDIX

Appendix A.

In this section, we prove formula (18). Substituting the SINR values from formulas (3) and (4) into formula (17), we have:

$$P_{out}^{VU_1}=1-\Pr\left(\frac{(1-\rho)\gamma_0\hat{g}_1}{\rho\gamma_0\hat{g}_1+a_1}\geq\gamma_{th2},\frac{\rho\gamma_0\hat{g}_1}{\kappa\gamma_0\hat{g}_1+a_1}>\gamma_{th1}\right) \quad \text{(A1)}$$

In the case $\gamma_{th2}>\frac{1-\rho}{\rho}$ or $\gamma_{th1}>\frac{\rho}{\kappa}$ then $P_{out}^{VU_1}=1$.

In the case $\gamma_{th2}<\frac{1-\rho}{\rho}\ \&\ \gamma_{th1}<\frac{\rho}{\kappa}$, we have:

$$P_{out}^{VU_1}=1-\Pr\left(\hat{g}_1\geq\varphi_1,\hat{g}_1\geq\varphi_2\right)=1-\Pr\left(\hat{g}_1>\underbrace{\max(\varphi_1,\varphi_2)}_{\varphi}\right)=F_{\hat{g}_1}(\varphi) \quad \text{(A2)}$$

Substituting formulas (13) and (15) into (A2), we get formula (18). It proved the Lemma 1.

Appendix B.

In this section, we prove formula (20). From (19), we have:

$$P_{out}^{VU_2}=\underbrace{\Pr\left(\gamma_2^{MRC}<\gamma_{th2}\right)}_{A}.\underbrace{\Pr\left(\gamma_1^{x_2}>\gamma_{th2}\right)}_{B}+\underbrace{\Pr\left(\gamma_1^{x_2}<\gamma_{th2},\gamma_2^{x_2}<\gamma_{th2}\right)}_{C} \quad \text{(B1)}$$

We continue to give the way to express A as follows:

$$A=\Pr\left(\frac{(1-\rho)\gamma_0\hat{g}_2}{\rho\gamma_0\hat{g}_2+a_2}+\frac{\gamma_0\hat{g}_3}{a_3}<\gamma_{th2}\right)=\Pr\left(\hat{g}_3<\varphi_3-\frac{(1-\rho)a_3\hat{g}_2}{\rho\gamma_0\hat{g}_2+a_2},\hat{g}_2<\varphi_4\right) \quad \text{(B2)}$$

where $\varphi_3=\frac{\gamma_{th2}a_3}{\gamma_0}$, $\gamma_4=\frac{a_2\gamma_{th2}}{\gamma_0(1-\rho-\rho\gamma_{th2})}$

For the TAS1 scheme, we rewrite (B2) as follows:

$$A=\int_0^{\varphi_4}F_{\hat{g}_2}\left[\varphi_3-\frac{(1-\rho)a_3\hat{g}_2}{\rho\gamma_0\hat{g}_2+a_2}\right]f_{\hat{g}_2}(x)dx$$

$$=\underbrace{\int_0^{\varphi_4}f_{\hat{g}_2}(x)dx}_{A_1}-\underbrace{\int_0^{\varphi_4}\sum_{i=0}^{m_3-1}\frac{\delta_3^i}{i!}\left[\varphi_3-\frac{(1-\rho)a_3x}{\rho\gamma_0x+a_2}\right]^i\exp\left(-\delta_3\left(\varphi_3-\frac{(1-\rho)a_3x}{\rho\gamma_0x+a_2}\right)\right)\frac{\delta_2^{m_2}x^{m_2-1}}{\Gamma(m_2)}\exp(-\delta_2x)dx}_{A_2}$$

We can quickly use formula (14) to calculate A_1 as follows.

$$A_1=1-\exp(-\delta_2\varphi_4)\sum_{i=0}^{m_2-1}\frac{(\delta_2\varphi_4)^i}{i!}$$

While A_2 is obtained using the Gaussian-Chebyshev quadrature method as follows:

$$A_2=\sum_{i=0}^{m_3-1}\frac{\delta_3^i}{i!}\frac{\delta_2^{m_2}}{\Gamma(m_2)}\int_0^{\varphi_4}\left[\varphi_3-\frac{(1-\rho)a_3x}{\rho\gamma_0x+a_2}\right]^i x^{m_2-1}\exp\left(-\delta_3\left(\varphi_3-\frac{(1-\rho)a_3x}{\rho\gamma_0x+a_2}\right)-\delta_2x\right)dx$$

$$=\sum_{i=0}^{m_3-1}\frac{\delta_3^i}{i!}\frac{\delta_2^{m_2}}{\Gamma(m_2)}\frac{\pi}{2Q}\varphi_4\sum_{q=1}^{Q}\left[\varphi_3-\frac{(1-\rho)a_3x_q}{\rho\gamma_0x_q+a_2}\right]^i x_q^{m_2-1}\exp\left(-\delta_3\left(\varphi_3-\frac{(1-\rho)a_3x_q}{\rho\gamma_0x_q+a_2}\right)-\delta_2x_q\right)\sqrt{1-\phi_i^2}$$

where $\phi_q=\cos\left(\frac{2q-1}{2Q}\pi\right)$, $x_q=\frac{\phi_q+1}{2}\varphi_4$, Q is the complexity-vs-accuracy trade-off coefficient.

After some algebra manipulations, we can quickly re-written the expressions B and C as follows:

$$B=\Pr\left(\gamma_1^{x_2}>\gamma_{th2}\right)=\Pr\left(\frac{(1-\rho)\gamma_0\hat{g}_1}{\rho\gamma_0\hat{g}_1+a_1}>\gamma_{th2}\right)=\begin{cases}0,\gamma_{th2}>\dfrac{1-\rho}{\rho}\\ 1-F_{\hat{g}_1}(\varphi_1),\gamma_{th2}<\dfrac{1-\rho}{\rho}\end{cases} \quad \text{(B3)}$$

$$C=\Pr\left(\gamma_1^{x_2}<\gamma_{th2},\gamma_2^{x_2}<\gamma_{th2}\right)=\begin{cases}1,\gamma_{th2}>\dfrac{1-\rho}{\rho}\\ F_{\hat{g}_1}(\varphi_1)F_{\hat{g}_2}(\varphi_4),\gamma_{th2}<\dfrac{1-\rho}{\rho}\end{cases} \quad \text{(B4)}$$

The proof of the formula for the TAS2 scheme is entirely similar. Thus, we have proved the formula for Lemma 2.